

Two-loop top-Yukawa-coupling corrections to the Higgs boson masses in the complex MSSM

Wolfgang Hollik and Sebastian Paßehr

*Max-Planck-Institut für Physik
(Werner-Heisenberg-Institut)
Föhringer Ring 6, D-80805 München, Germany*

Results for the leading two-loop corrections of $\mathcal{O}(\alpha_t^2)$ from the Yukawa sector to the Higgs-boson masses of the MSSM with complex parameters are presented. The corresponding self-energies and their renormalization have been obtained in a Feynman-diagrammatic approach. A numerical analysis of the new contributions is performed for the mass of the lightest Higgs boson, supplemented by the full one-loop result and the $\mathcal{O}(\alpha_t\alpha_s)$ terms including complex phases. In the limit of the real MSSM a previous result is confirmed.

1 Introduction

The discovery of a new boson [1, 2] with a mass around 125.6 GeV by the experiments ATLAS and CMS at CERN has triggered an intensive investigation to reveal the nature of this particle as a Higgs boson from the mechanism of electroweak symmetry breaking. Within the present experimental uncertainties, which are still considerably large, the measured properties of the new boson are consistent with the corresponding predictions for the Standard Model Higgs boson [3], but still a large variety of other interpretations is possible which are connected to physics beyond the Standard Model. Within the theoretical well motivated minimal supersymmetric Standard Model (MSSM), the observed particle could be classified as a light state within a richer predicted spectrum. The Higgs sector of the MSSM consists of two complex scalar doublets leading to five physical Higgs bosons and three (would-be) Goldstone bosons. At the tree-level, the physical states are given by the neutral CP -even h, H and CP -odd A bosons, together with the charged H^\pm bosons, and can be parametrized in terms of the A -boson mass m_A and the ratio of the two vacuum expectation values, $\tan\beta = v_2/v_1$. In the MSSM with complex parameters, the cMSSM, CP violation is induced in the Higgs sector by loop contributions with complex parameters from other SUSY sectors leading to mixing between h, H and A in the mass eigenstates [4].

Masses and mixings in the neutral sector are sizeably influenced by loop contributions, and accordingly intensive work has been invested into higher-order calculations of the mass spectrum from the SUSY parameters, in the case of the real MSSM [5–16] as well as the cMSSM [17–20]. The largest loop contributions arise from the Yukawa sector with the large top Yukawa coupling h_t , or $\alpha_t = h_t^2/(4\pi)$, respectively. The class of leading two-loop Yukawa-type corrections of $\mathcal{O}(\alpha_t^2)$ has been calculated so far only in the case of real parameters [11, 12], applying the effective-potential method. Together with the full one-loop result [21] and the leading $\mathcal{O}(\alpha_t\alpha_s)$ terms [20], both accomplished in the Feynman-diagrammatic approach including complex parameters, it has been implemented in the public program **FeynHiggs** [7, 13, 21–23]. A calculation of the $\mathcal{O}(\alpha_t^2)$ terms for the cMSSM, however, has been missing until now.

In this letter we present this class of $\mathcal{O}(\alpha_t^2)$ contributions extended to the case of complex parameters. The computation has been carried out in the Feynman-diagrammatic approach; for the special case of real parameters we obtain a result equivalent to the one in [12] in an independent way, serving thus as a cross check and as a consolidation of former spectrum calculations and associated tools. These new contributions will be included in the code **FeynHiggs**.

2 Higgs boson masses in the cMSSM

2.1 Tree-level relations

The two scalar $SU(2)$ doublets can be decomposed according to

$$\mathcal{H}_1 = \begin{pmatrix} H_{11} \\ H_{12} \end{pmatrix} = \begin{pmatrix} v_1 + \frac{1}{\sqrt{2}}(\phi_1 - i\chi_1) \\ -\phi_1^- \end{pmatrix}, \quad \mathcal{H}_2 = \begin{pmatrix} H_{21} \\ H_{22} \end{pmatrix} = e^{i\xi} \begin{pmatrix} \phi_2^+ \\ v_2 + \frac{1}{\sqrt{2}}(\phi_2 + i\chi_2) \end{pmatrix}, \quad (2.1)$$

leading to the Higgs potential written as an expansion in terms of the components [with the notation $\phi_1^- = (\phi_1^+)^\dagger$, $\phi_2^- = (\phi_2^+)^\dagger$],

$$V_H = -T_{\phi_1}\phi_1 - T_{\phi_2}\phi_2 - T_{\chi_1}\chi_1 - T_{\chi_2}\chi_2 \\ + \frac{1}{2}(\phi_1, \phi_2, \chi_1, \chi_2) \begin{pmatrix} \mathbf{M}_\phi & \mathbf{M}_{\phi\chi} \\ \mathbf{M}_{\phi\chi}^\dagger & \mathbf{M}_\chi \end{pmatrix} \begin{pmatrix} \phi_1 \\ \phi_2 \\ \chi_1 \\ \chi_2 \end{pmatrix} + (\phi_1^-, \phi_2^-) \mathbf{M}_{\phi^\pm} \begin{pmatrix} \phi_1^+ \\ \phi_2^+ \end{pmatrix} + \dots, \quad (2.2)$$

where higher powers in field components have been dropped. The explicit form of the tadpole coefficients T_i and of the mass matrices \mathbf{M} can be found in Ref. [21]. They are parametrized by the phase ξ , the real SUSY breaking quantities $m_{1,2}^2 = \tilde{m}_{1,2}^2 + |\mu|^2$, and the complex SUSY breaking quantity m_{12}^2 . The latter can be redefined as real [24] with the help of a Peccei–Quinn transformation [25] leaving only the phase ξ as a source of CP violation at the tree-level. The requirement of minimizing V_H at the vacuum expectation values v_1 and v_2 induces vanishing tadpoles at tree level, which in turn leads to $\xi = 0$. As a consequence, also $\mathbf{M}_{\phi\chi}$ is equal to zero and $\phi_{1,2}$ are decoupled from $\chi_{1,2}$ at the tree-level. The remaining 2×2 matrices $\mathbf{M}_\phi, \mathbf{M}_\chi, \mathbf{M}_{\phi^\pm}$ can be transformed into the mass eigenstate basis with the help of unitary matrices $D(x) = \begin{pmatrix} -s_x & c_x \\ c_x & s_x \end{pmatrix}$, writing $s_x \equiv \sin x$ and $c_x \equiv \cos x$:

$$\begin{pmatrix} h \\ H \end{pmatrix} = D(\alpha) \begin{pmatrix} \phi_1 \\ \phi_2 \end{pmatrix}, \quad \begin{pmatrix} A \\ G \end{pmatrix} = D(\beta) \begin{pmatrix} \chi_1 \\ \chi_2 \end{pmatrix}, \quad \begin{pmatrix} H^\pm \\ G^\pm \end{pmatrix} = D(\beta) \begin{pmatrix} \phi_1^\pm \\ \phi_2^\pm \end{pmatrix}. \quad (2.3)$$

The Higgs potential in this basis can be expressed as follows,

$$\begin{aligned} V_H = & -T_h h - T_H H - T_A A - T_G G \\ & + \frac{1}{2} (h, H, A, G) \mathbf{M}_{hHAG} \begin{pmatrix} h \\ H \\ A \\ G \end{pmatrix} + (H^-, G^-) \mathbf{M}_{H^\pm G^\pm} \begin{pmatrix} H^+ \\ G^+ \end{pmatrix} + \dots \end{aligned} \quad (2.4)$$

with the tadpole coefficients and mass matrices as given in [21]. At lowest order, the tadpoles vanish and the mass matrices $\mathbf{M}_{hHAG}^{(0)} = \text{diag}(m_h^2, m_H^2, m_A^2, m_G^2)$, $\mathbf{M}_{H^\pm G^\pm}^{(0)} = \text{diag}(m_{H^\pm}^2, m_{G^\pm}^2)$ are diagonal.

2.2 Mass spectrum beyond lowest order

At higher order, the entries of the Higgs boson mass matrices are shifted according to the self-energies, yielding in general mixing of all tree-level mass eigenstates with equal quantum numbers. In the case of the neutral Higgs bosons the following “mass matrix” is evaluated at the two-loop level,

$$\mathbf{M}_{hHAG}^{(2)}(p^2) = \mathbf{M}_{hHAG}^{(0)} - \hat{\Sigma}_{hHAG}^{(1)}(p^2) - \hat{\Sigma}_{hHAG}^{(2)}(0). \quad (2.5)$$

Therein, $\hat{\Sigma}_{hHAG}^{(k)}$ denotes the matrix of the renormalized diagonal and non-diagonal self-energies for the h, H, A, G fields at loop order k . The present approximation for the two-loop part yielding the leading contributions from the Yukawa sector, treats the two-loop self-energies at $p^2 = 0$ for the external momentum (as done also for the leading two-loop $\mathcal{O}(\alpha_t \alpha_s)$ contributions [20]) and neglects contributions from the gauge sector (gaugeless limit). Furthermore, also the Yukawa coupling of the bottom quark is neglected by setting the b -quark mass to zero. The diagrammatic calculation of the self-energies has been performed with **FeynArts** [27] for the generation of the Feynman diagrams and **TwoCalc** [28] for the two-loop tensor reduction and trace evaluation. The renormalization constants have been obtained with the help of **FormCalc** [29].

In order to obtain the physical Higgs-boson masses from the dressed propagators in the considered approximation, it is sufficient to derive explicitly the entries of the 3×3 submatrix of Eq. (2.5) corresponding to the (hHA) components. Mixing with the unphysical Goldstone boson yields subleading two-loop contributions; also Goldstone– Z mixing occurs in principle, which is related to the other Goldstone mixings by Slavnov–Taylor identities [30, 31] and of subleading type as well [26]. However, A – G mixing has to be taken into account in intermediate steps for a consistent renormalization.

The masses of the three neutral Higgs bosons h_1, h_2, h_3 , including the new $\mathcal{O}(\alpha_t^2)$ contributions, are given by the real parts of the poles of the hHA propagator matrix, obtained as the zeroes of the determinant of the renormalized two-point vertex function,

$$\det \hat{\Gamma}_{hHA}(p^2) = 0, \quad \hat{\Gamma}_{hHA}(p^2) = i \left[p^2 \mathbf{1} - \mathbf{M}_{hHA}^{(2)}(p^2) \right], \quad (2.6)$$

involving the corresponding 3×3 submatrix of Eq. (2.5).

2.3 Two-loop renormalization

For obtaining the renormalized self-energies (2.5), counterterms have to be introduced for the mass matrices and tadpoles in Eq. (2.4) up to second order in the loop expansion,

$$\mathbf{M}_{hHAG} \rightarrow \mathbf{M}_{hHAG}^{(0)} + \delta^{(1)} \mathbf{M}_{hHAG} + \delta^{(2)} \mathbf{M}_{hHAG}, \quad (2.7a)$$

$$\mathbf{M}_{H^\pm G^\pm} \rightarrow \mathbf{M}_{H^\pm G^\pm}^{(0)} + \delta^{(1)} \mathbf{M}_{H^\pm G^\pm} + \delta^{(2)} \mathbf{M}_{H^\pm G^\pm}, \quad (2.7b)$$

$$T_i \rightarrow T_i + \delta^{(1)} T_i + \delta^{(2)} T_i, \quad i = h, H, A, G, \quad (2.7c)$$

as well as field renormalization constants $Z_{\mathcal{H}_i} = 1 + \delta^{(1)} Z_{\mathcal{H}_i} + \delta^{(2)} Z_{\mathcal{H}_i}$, which are introduced up to two-loop order for each of the scalar doublets in Eq. (2.1) through

$$\mathcal{H}_i \rightarrow \sqrt{Z_{\mathcal{H}_i}} \mathcal{H}_i = \left[1 + \frac{1}{2} \delta^{(1)} Z_{\mathcal{H}_i} + \frac{1}{2} \delta^{(2)} Z_{\mathcal{H}_i} - \frac{1}{8} \left(\delta^{(1)} Z_{\mathcal{H}_i} \right)^2 \right] \mathcal{H}_i. \quad (2.8)$$

They can be transformed into (dependent) field-renormalization constants for the mass eigenstates in Eq. (2.3) according to

$$\begin{pmatrix} h \\ H \end{pmatrix} \rightarrow D(\alpha) \begin{pmatrix} \sqrt{Z_{\mathcal{H}_1}} & 0 \\ 0 & \sqrt{Z_{\mathcal{H}_2}} \end{pmatrix} D(\alpha)^{-1} \begin{pmatrix} h \\ H \end{pmatrix} \equiv \mathbf{Z}_{hH} \begin{pmatrix} h \\ H \end{pmatrix}, \quad (2.9a)$$

$$\begin{pmatrix} A \\ G \end{pmatrix} \rightarrow D(\beta) \begin{pmatrix} \sqrt{Z_{\mathcal{H}_1}} & 0 \\ 0 & \sqrt{Z_{\mathcal{H}_2}} \end{pmatrix} D(\beta)^{-1} \begin{pmatrix} A \\ G \end{pmatrix} \equiv \mathbf{Z}_{AG} \begin{pmatrix} A \\ G \end{pmatrix}, \quad (2.9b)$$

$$\begin{pmatrix} H^\pm \\ G^\pm \end{pmatrix} \rightarrow D(\beta) \begin{pmatrix} \sqrt{Z_{\mathcal{H}_1}} & 0 \\ 0 & \sqrt{Z_{\mathcal{H}_2}} \end{pmatrix} D(\beta)^{-1} \begin{pmatrix} H^\pm \\ G^\pm \end{pmatrix} \equiv \mathbf{Z}_{H^\pm G^\pm} \begin{pmatrix} H^\pm \\ G^\pm \end{pmatrix}. \quad (2.9c)$$

At the one-loop level, the expressions for the counterterms and for the renormalized self-energies $\hat{\Sigma}_{hHAG}^{(1)}(p^2)$ are listed in [21]. For the leading two-loop contributions, we have to evaluate the renormalized two-loop self energies at zero external momentum. In compact matrix notation they can be written as follows,

$$\hat{\Sigma}_{hHAG}^{(2)}(0) = \Sigma_{hHAG}^{(2)}(0) - \delta^{(2)} \mathbf{M}_{hHAG}^Z. \quad (2.10)$$

Thereby, $\Sigma_{hHAG}^{(2)}$ denotes the unrenormalized self-energies corresponding to the genuine 2-loop diagrams and diagrams with sub-renormalization, as illustrated in Fig. 1. The quantities in $\delta^{(2)} \mathbf{M}_{hHAG}^Z$ can be obtained as the two-loop content of the expression

$$\delta^{(2)} \mathbf{M}_{hHAG}^Z = \begin{pmatrix} \mathbf{Z}_{hH}^T & \mathbf{0} \\ \mathbf{0} & \mathbf{Z}_{AG}^T \end{pmatrix} \left(\mathbf{M}_{hHAG}^{(0)} + \delta^{(1)} \mathbf{M}_{hHAG} + \delta^{(2)} \mathbf{M}_{hHAG} \right) \begin{pmatrix} \mathbf{Z}_{hH} & \mathbf{0} \\ \mathbf{0} & \mathbf{Z}_{AG} \end{pmatrix}. \quad (2.11)$$

Explicit formulae will be given in a forthcoming paper.

The entries of the counterterm matrices in Eq. (2.10) are determined via renormalization conditions that are extended from the one-loop level, as specified in [21], to two-loop order:

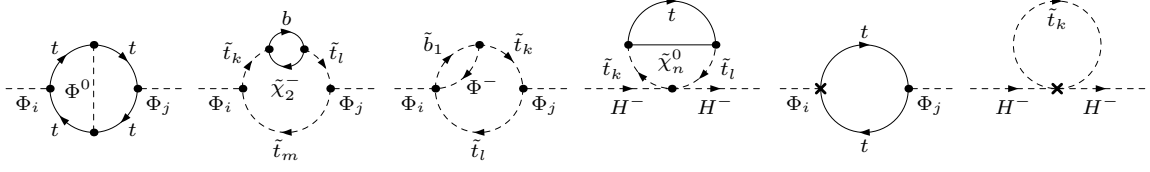


Figure 1. Examples of two-loop self-energy diagrams. The cross denotes a one-loop counterterm insertion. $\Phi_i = h, H, A$; $\Phi^0 = h, H, A, G$; $\Phi^- = H^-, G^-$.

- The tadpole counterterms $\delta^{(k)}T_i$ are fixed by requiring the minimum of the Higgs potential not shifted, *i. e.*¹

$$T_i^{(1)} + \delta^{(1)}T_i = 0, \quad T_i^{(2)} + \delta^{(2)}T_i + \delta^{(2)}T_i^Z = 0, \quad i = h, H, A, \quad (2.12a)$$

with

$$\left(\delta^{(2)}T_h^Z, \delta^{(2)}T_H^Z\right) = \left(\delta^{(1)}T_h, \delta^{(1)}T_H\right) \mathbf{Z}_{hH}, \quad (2.12b)$$

$$\left(\delta^{(2)}T_A^Z, \delta^{(2)}T_G^Z\right) = \left(\delta^{(1)}T_A, \delta^{(1)}T_G\right) \mathbf{Z}_{AG}, \quad (2.12c)$$

where only the one-loop parts of the \mathbf{Z}_{ij} from Eq. (2.9) are involved. $T_i^{(k)}$ denote the unrenormalized one-point vertex functions; two-loop diagrams contributing to $T_i^{(2)}$ are displayed in Fig. 2.

- The charged Higgs-boson mass m_{H^\pm} is the only independent mass parameter of the Higgs sector and is used as an input quantity. Accordingly, the corresponding mass counterterm is fixed by an independent renormalization condition, chosen as on-shell condition, which in the $p^2 = 0$ approximation is given by $\Re \hat{\Sigma}_{H^\pm}^{(k)}(0) = 0$ for the renormalized charged-Higgs self-energy, at the two-loop level specified in terms of the unrenormalized charged self-energies and respective counterterms,

$$\hat{\Sigma}_{H^\pm}^{(2)} = \left(\hat{\Sigma}_{H^\pm G^\pm}^{(2)}\right)_{11}, \quad \hat{\Sigma}_{H^\pm G^\pm}^{(2)}(0) = \Sigma_{H^\pm G^\pm}^{(2)}(0) - \delta^{(2)}\mathbf{M}_{H^\pm G^\pm}^Z, \quad (2.13a)$$

$$\delta^{(2)}\mathbf{M}_{H^\pm G^\pm}^Z = \mathbf{Z}_{H^\pm G^\pm}^T \left(\mathbf{M}_{H^\pm G^\pm}^{(0)} + \delta^{(1)}\mathbf{M}_{H^\pm G^\pm} + \delta^{(2)}\mathbf{M}_{H^\pm G^\pm}\right) \mathbf{Z}_{H^\pm G^\pm}, \quad (2.13b)$$

where only the two-loop content of the last expression is taken. From the on-shell condition, the independent mass counterterm $\delta^{(2)}m_{H^\pm}^2 = (\delta^{(2)}\mathbf{M}_{H^\pm G^\pm})_{11}$ can be extracted.

- The field-renormalization constants of the Higgs mass eigenstates in Eq. (2.9) are combinations of the basic doublet-field renormalization constants $\delta^{(k)}Z_{\mathcal{H}_1}$ and $\delta^{(k)}Z_{\mathcal{H}_2}$ ($k = 1, 2$), which are fixed by the \overline{DR} conditions for the derivatives of the corresponding self-energies,

$$\delta^{(k)}Z_{\mathcal{H}_1} = -\left[\Sigma_{HH}^{(k)'}(0)\right]_{\alpha=0}^{\text{div}}, \quad \delta^{(k)}Z_{\mathcal{H}_2} = -\left[\Sigma_{hh}^{(k)'}(0)\right]_{\alpha=0}^{\text{div}}. \quad (2.14)$$

- $t_\beta \equiv \tan \beta$ is renormalized in the \overline{DR} scheme, which has been shown to be a very convenient choice [32] (alternative process-dependent definitions and renormalization of t_β can be found in Ref. [30]). It has been clarified in Ref. [33, 34] that the following identity applies for the \overline{DR} counterterm at one-loop order and within our approximations also at the two-loop level:

$$\delta^{(k)}t_\beta = \frac{1}{2}t_\beta \left(\delta^{(k)}Z_{\mathcal{H}_2} - \delta^{(k)}Z_{\mathcal{H}_1}\right). \quad (2.15)$$

¹The counterterms $\delta^{(k)}T_G$ are not independent and do not need separate renormalization conditions

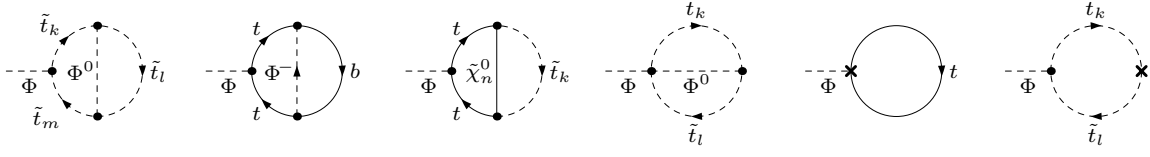


Figure 2. Examples of two-loop tadpole diagrams contributing to $T_i^{(2)}$. The cross denotes a one-loop counterterm insertion. $\Phi_i = h, H, A$; $\Phi^0 = h, H, A, G$; $\Phi^- = H^-, G^-$.

- In the on-shell scheme, also the counterterms $\delta M_W^2/M_W^2$ and $\delta M_Z^2/M_Z^2$ are required for renormalization of the top Yukawa coupling $h_t = (em_t)/(\sqrt{2}s_\beta s_w M_W)$. In the gaugeless limit these ratios have remaining finite and divergent contributions arising from the Yukawa couplings, which have to be included as one-loop quantities $\sim h_t^2$; they are evaluated from the W and Z self-energies yielding

$$\frac{\delta M_W^2}{M_W^2} = \frac{\Sigma_W(0)}{M_W^2}, \quad \frac{\delta M_Z^2}{M_Z^2} = \frac{\Sigma_Z(0)}{M_Z^2}, \quad \delta s_w^2 = c_w^2 \left(\frac{\delta M_Z^2}{M_Z^2} - \frac{\delta M_W^2}{M_W^2} \right). \quad (2.16)$$

In the Yukawa approximation, δs_w^2 is finite. The corresponding Feynman graphs are depicted in Fig. 4.

As a consequence of applying \overline{DR} renormalization conditions the result depends explicitly on the renormalization scale. Conventionally it is chosen as m_t being the default value in **FeynHiggs**.

The appearance of δs_w^2 in the $\mathcal{O}(\alpha_t^2)$ terms, as specified above, is a consequence of the on-shell scheme where the top-Yukawa coupling $h_t = m_t/v_2 = m_t/(vs_\beta)$ is expressed in terms of

$$\frac{1}{v} = \frac{g_2}{\sqrt{2}M_W} = \frac{e}{\sqrt{2}s_w M_W}. \quad (2.17)$$

Accordingly, the one-loop self-energies have to be parametrized in terms of this representation for h_t when added to the two-loop self-energies in Eq. (2.5). On the other hand, if the Fermi constant G_F is used for parametrization of the one-loop self-energies, the relation

$$\sqrt{2}G_F = \frac{e^2}{4s_w^2 M_W^2} \left(1 + \Delta^{(k)} r \right), \quad (2.18)$$

has to be applied, which gets loop contributions also in the gaugeless limit, at one-loop order given by

$$\Delta^{(1)} r = -\frac{c_w^2}{s_w^2} \left(\frac{\delta M_Z^2}{M_Z^2} - \frac{\delta M_W^2}{M_W^2} \right) = -\frac{\delta s_w^2}{s_w^2}. \quad (2.19)$$

This finite shift in the one-loop self-energies induces two-loop $\mathcal{O}(\alpha_t^2)$ terms and has to be taken into account, effectively cancelling all occurrences of δs_w^2 .

3 Colored-sector input and renormalization

The two-loop top Yukawa coupling contributions to the self-energies and tadpoles involve insertions of counterterms that arise from one-loop renormalization of the top and scalar top (\tilde{t}) as well as scalar bottom (\tilde{b}) sectors. The stop and sbottom mass matrices in the $(\tilde{t}_L, \tilde{t}_R)$ and $(\tilde{b}_L, \tilde{b}_R)$ bases are given by

$$\mathbf{M}_{\tilde{q}} = \begin{pmatrix} m_{\tilde{q}L}^2 + m_q^2 + M_Z^2 c_{2\beta} (T_q^3 - Q_q s_w^2) & m_q (A_q^* - \mu \kappa_q) \\ m_q (A_q - \mu^* \kappa_q) & m_{\tilde{q}R}^2 + m_q^2 + M_Z^2 c_{2\beta} Q_q s_w^2 \end{pmatrix}, \quad \kappa_t = \frac{1}{t_\beta}, \quad \kappa_b = t_\beta, \quad (3.1)$$

with Q_q and T_q^3 denoting charge and isospin of $q = t, b$. $SU(2)$ invariance requires $m_{\tilde{t}_L}^2 = m_{\tilde{b}_L}^2 \equiv m_{\tilde{q}_3}^2$. In the gaugeless approximation the D -terms vanish in both the \tilde{t} and \tilde{b} matrices. Moreover, in our approximation the b -quark is treated as massless; hence, the off-diagonal entries of the sbottom matrix are zero and the mass eigenvalues can be read off directly, $m_{\tilde{t}_1}^2 = m_{\tilde{b}_L}^2 = m_{\tilde{q}_3}^2$, $m_{\tilde{t}_2}^2 = m_{\tilde{b}_R}^2$. The stop mass eigenvalues can be obtained by performing a unitary transformation,

$$\mathbf{U}_{\tilde{t}} \mathbf{M}_{\tilde{t}} \mathbf{U}_{\tilde{t}}^\dagger = \text{diag}(m_{\tilde{t}_1}^2, m_{\tilde{t}_2}^2). \quad (3.2)$$

Since A_t and μ are complex parameters in general, the unitary matrix $\mathbf{U}_{\tilde{t}}$ consists of one mixing angle $\theta_{\tilde{t}}$ and one phase $\varphi_{\tilde{t}}$.

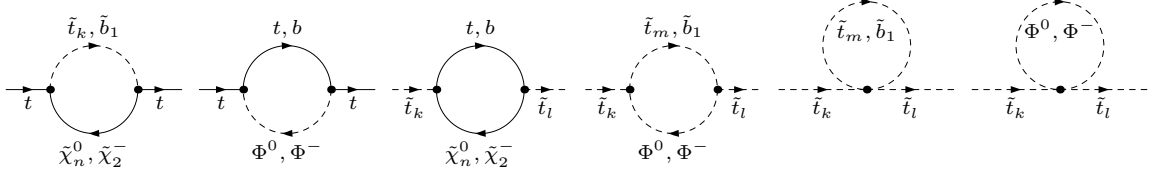


Figure 3. Feynman diagrams for renormalization of the quark-squark sector. $\Phi^0 = h^0, H^0, A^0, G^0$; $\Phi^- = H^-, G^-$.

Five independent parameters are introduced by the quark-squark sector, which enter the two-loop calculation in addition to those of the previous section: the top mass m_t , the soft SUSY-breaking parameters $m_{\tilde{q}_3}$ and $m_{\tilde{t}_R}$ ($m_{\tilde{b}_R}$ decouples for $m_b = 0$), and the complex mixing parameter $A_t = |A_t|e^{i\phi_{A_t}}$. On top, μ enters as another free parameter related to the Higgsino sector. These parameters have to be renormalized at the one-loop level,

$$m_t \rightarrow m_t + \delta m_t, \quad \mathbf{M}_{\tilde{t}} \rightarrow \mathbf{M}_{\tilde{t}} + \delta \mathbf{M}_{\tilde{t}}. \quad (3.3)$$

The independent renormalization conditions for the colored sector are formulated in the following way:

- The mass of the top quark is defined on-shell, *i.e.*²

$$\delta m_t = \frac{1}{2} m_t \Re [\Sigma_t^L(m_t^2) + \Sigma_t^R(m_t^2) + 2\Sigma_t^S(m_t^2)], \quad (3.4)$$

according to the Lorentz decomposition of the self-energy of the top quark (Fig. 3)

$$\Sigma_t(p) = \not{p} \omega_- \Sigma_t^L(p^2) + \not{p} \omega_+ \Sigma_t^R(p^2) + m_t \Sigma_t^S(p^2) + m_t \gamma_5 \Sigma_t^{PS}(p^2). \quad (3.5)$$

- $m_{\tilde{q}_3}^2$ and $m_{\tilde{t}_R}^2$ are traded for $m_{\tilde{t}_1}^2$ and $m_{\tilde{t}_2}^2$, which are then fixed by on-shell conditions for the top-squarks,

$$\delta m_{\tilde{t}_i}^2 = \Re \Sigma_{\tilde{t}_{ii}}(m_{\tilde{t}_i}^2), \quad i = 1, 2, \quad (3.6)$$

involving the diagonal \tilde{t}_1 and \tilde{t}_2 self-energies (diagrammatically visualized in Fig. 3). These on-shell conditions determine the diagonal entries of the counterterm matrix

$$\mathbf{U}_{\tilde{t}} \delta \mathbf{M}_{\tilde{t}} \mathbf{U}_{\tilde{t}}^\dagger = \begin{pmatrix} \delta m_{\tilde{t}_1}^2 & \delta m_{\tilde{t}_1 \tilde{t}_2}^2 \\ \delta m_{\tilde{t}_1 \tilde{t}_2}^{2*} & \delta m_{\tilde{t}_2}^2 \end{pmatrix}. \quad (3.7)$$

² \Re denotes the real part of all loop integrals, but leaves the couplings unaffected.

- The mixing parameter A_t is correlated with the \tilde{t} -mass eigenvalues, t_β , and μ , through Eq. (3.2). Exploiting Eq. (3.7) and the unitarity of $\mathbf{U}_{\tilde{t}}$ yields the expression

$$\left(A_t - \frac{\mu^*}{t_\beta}\right) \delta m_t + m_t \left(\delta A_t - \frac{\delta \mu^*}{t_\beta} + \frac{\mu^* \delta t_\beta}{t_\beta^2}\right) = \mathbf{U}_{\tilde{t}11} \mathbf{U}_{\tilde{t}12}^* \left(\delta m_{\tilde{t}_1}^2 - \delta m_{\tilde{t}_2}^2\right) + \mathbf{U}_{\tilde{t}21} \mathbf{U}_{\tilde{t}12}^* \delta m_{\tilde{t}_1 \tilde{t}_2}^2 + \mathbf{U}_{\tilde{t}22} \mathbf{U}_{\tilde{t}11}^* \delta m_{\tilde{t}_1 \tilde{t}_2}^{2*}. \quad (3.8)$$

For the non-diagonal entry of (3.7), the renormalization condition

$$\delta m_{\tilde{t}_1 \tilde{t}_2}^2 = \frac{1}{2} \Re \left[\Sigma_{\tilde{t}12} \left(m_{\tilde{t}_1}^2 \right) + \Sigma_{\tilde{t}12} \left(m_{\tilde{t}_2}^2 \right) \right] \quad (3.9)$$

is imposed, as in [20], which involves the non-diagonal \tilde{t}_1 – \tilde{t}_2 self-energy (Fig. 3). By means of Eq. (3.8) the counterterm δA_t is then determined. Actually this yields two conditions, for $|A_t|$ and for the phase ϕ_{A_t} separately. The additionally required mass counterterm $\delta \mu$ is obtained as described below in section 4.

- As already mentioned, the relevant sbottom mass is not an independent parameter, and hence its counterterm is a derived quantity that can be obtained from Eq. (3.7),

$$\delta m_{b_1}^2 \equiv \delta m_{q_3}^2 = |\mathbf{U}_{\tilde{t}11}|^2 \delta m_{\tilde{t}_1}^2 + |\mathbf{U}_{\tilde{t}12}|^2 \delta m_{\tilde{t}_2}^2 - \mathbf{U}_{\tilde{t}22} \mathbf{U}_{\tilde{t}12}^* \delta m_{\tilde{t}_1 \tilde{t}_2}^2 - \mathbf{U}_{\tilde{t}12} \mathbf{U}_{\tilde{t}22}^* \delta m_{\tilde{t}_1 \tilde{t}_2}^{2*} - 2m_t \delta m_t. \quad (3.10)$$

4 Chargino–neutralino-sector input and renormalization

For the calculation of the $\mathcal{O}(\alpha_t^2)$ contributions to the Higgs boson self-energies and tadpoles, also the neutralino and chargino sectors have to be considered. Chargino/neutralino vertices and propagators enter only at the two-loop level and thus do not need renormalization; in the one-loop terms, however, the Higgsino-mass parameter μ appears and the counterterm $\delta \mu$ is required for the one-loop subrenormalization. The mass matrices in the bino/wino/higgsino bases are given by

$$\mathbf{Y} = \begin{pmatrix} M_1 & 0 & -M_Z s_w c_\beta & M_Z s_w s_\beta \\ 0 & M_2 & M_Z c_w c_\beta & M_Z c_w s_\beta \\ -M_Z s_w c_\beta & M_Z c_w c_\beta & 0 & -\mu \\ M_Z s_w s_\beta & M_Z c_w s_\beta & -\mu & 0 \end{pmatrix} \quad \text{and} \quad \mathbf{X} = \begin{pmatrix} M_2 & \sqrt{2} M_W s_\beta \\ \sqrt{2} M_W c_\beta & \mu \end{pmatrix}. \quad (4.1)$$

Diagonal matrices with real and positive entries are obtained with the help of unitary matrices $\mathbf{N}, \mathbf{U}, \mathbf{V}$ by the transformations

$$\mathbf{N}^* \mathbf{Y} \mathbf{N}^\dagger = \text{diag} \left(m_{\tilde{\chi}_1^0}, m_{\tilde{\chi}_2^0}, m_{\tilde{\chi}_3^0}, m_{\tilde{\chi}_4^0} \right), \quad \mathbf{U}^* \mathbf{X} \mathbf{V}^\dagger = \text{diag} \left(m_{\tilde{\chi}_1^\pm}, m_{\tilde{\chi}_2^\pm} \right). \quad (4.2)$$

In the gaugeless limit the off-diagonal (2×2) blocks of \mathbf{Y} and the off-diagonal entries of \mathbf{X} vanish. For this special case the transformation matrices and diagonal entries in Eq. (4.2) simplify,

$$\mathbf{N} = \begin{pmatrix} e^{\frac{i}{2} \phi_{M_1}} & 0 & 0 \\ 0 & e^{\frac{i}{2} \phi_{M_2}} & 0 \\ 0 & 0 & \frac{1}{\sqrt{2}} e^{\frac{i}{2} \phi_\mu} \begin{pmatrix} 1 & -1 \\ i & i \end{pmatrix} \end{pmatrix}, \quad \mathbf{U} = \begin{pmatrix} e^{i \phi_{M_2}} & 0 \\ 0 & e^{i \phi_\mu} \end{pmatrix}, \quad \mathbf{V} = \mathbf{1}; \quad (4.3a)$$

$$m_{\tilde{\chi}_1^0} = |M_1|, \quad m_{\tilde{\chi}_2^0} = |M_2|, \quad m_{\tilde{\chi}_3^0} = |\mu|, \quad m_{\tilde{\chi}_4^0} = |\mu|, \quad m_{\tilde{\chi}_1^\pm} = |M_2|, \quad m_{\tilde{\chi}_2^\pm} = |\mu|; \quad (4.3b)$$

and only the Higgsinos $\tilde{\chi}_3^0, \tilde{\chi}_4^0, \tilde{\chi}_2^\pm$ remain in the $\mathcal{O}(\alpha_t^2)$ contributions.

The Higgsino mass parameter μ is an independent input quantity and has to be renormalized accordingly, $\mu \rightarrow \mu + \delta\mu$, fixing the counterterm $\delta\mu$ by an independent renormalization condition, which renders the one-loop subrenormalization complete. Together with the soft-breaking parameters M_1 and M_2 , μ can be defined in the neutralino/chargino sector by requiring on-shell conditions for the two charginos and one neutralino. However, since only $\delta\mu$ is required here, it is sufficient to impose a renormalization condition for $\tilde{\chi}_2^\pm$ only; the appropriate on-shell condition reads,

$$\delta\mu = \frac{1}{2}e^{i\phi_\mu} \left\{ |\mu| \Re \left[\Sigma_{\tilde{\chi}_2^\pm}^L(|\mu|^2) + \Sigma_{\tilde{\chi}_2^\pm}^R(|\mu|^2) \right] + 2\Re \left[\Sigma_{\tilde{\chi}_2^\pm}^S(|\mu|^2) \right] \right\}, \quad (4.4)$$

where the Lorentz decomposition of the self-energy for the Higgsino-like chargino $\tilde{\chi}_2^\pm$ (see Fig. 4) has been applied, in analogy to Eq. (3.5).

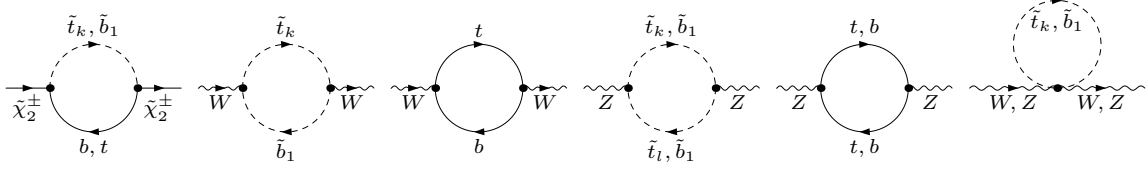


Figure 4. Feynman diagrams for the counterterms $\delta\mu$, $\delta M_W/M_W$, and $\delta M_Z/M_Z$.

Another option implemented in the $\mathcal{O}(\alpha_t^2)$ result is the \overline{DR} renormalization of μ , which defines the counterterm $\delta\mu$ in the \overline{DR} scheme, *i.e.* by the divergent part of the expression in Eq. (4.4). For the numerical analysis and comparison with [12] the \overline{DR} scheme is chosen at the scale m_t .

5 Numerical analysis

In this section we focus on the lightest Higgs-boson mass derived from Eq. (2.6) and present results for m_{h_1} in different parameter scenarios. In each case the complete one-loop results and the $\mathcal{O}(\alpha_t \alpha_s)$ terms are obtained from **FeynHiggs**, while the $\mathcal{O}(\alpha_t^2)$ terms are computed by means of the corresponding two-loop self-energies specified in the previous sections with the parameters μ, t_β and the Higgs field-renormalization constants defined in the \overline{DR} scheme at the scale m_t . Thereby, the new $\mathcal{O}(\alpha_t^2)$ self-energies are combined with the results of the other available self-energies according to Eq. (2.5) within **FeynHiggs**, and the masses are derived via Eq. (2.6). For comparison with previous results G_F is chosen for normalization as mentioned at the end of section 2.3.

The input parameters for the numerical results in this section are shown in the figures or the captions, respectively, when they are varied. The residual parameters, being the same for all the plots, are chosen as $M_2 = 200$ GeV, $M_1 = (5s_w^2)/(3c_w^2) M_2$, and $m_{\tilde{t}_L} = m_{\tilde{q}_L} = m_{\tilde{t}_R} = m_{\tilde{q}_R} = 2000$ GeV for the first two sfermion generations, together with the Standard Model input $m_t = 173.2$ GeV and $\alpha_s = 0.118$.

As a first application, we study the case of the real MSSM, where an analytic result of the $\mathcal{O}(\alpha_t^2)$ contributions is known [12] from a calculation making use of the effective-potential method. The version of **FeynHiggs** for real parameters has this result included, making thus a direct comparison with the prediction of our new diagrammatic calculation possible. Thereby all parameters and the renormalization have been adapted to agree with Ref. [12]. Very good agreement is found between the two results that have been obtained in completely independent ways. As an example, this feature is displayed in Fig. 5, where the shift from the $\mathcal{O}(\alpha_t^2)$ terms in the two approaches are shown on top of the mass prediction without those terms. The grey band depicts the mass range 125.6 ± 1 GeV around the Higgs signal measured by ATLAS and CMS. The mass shifts

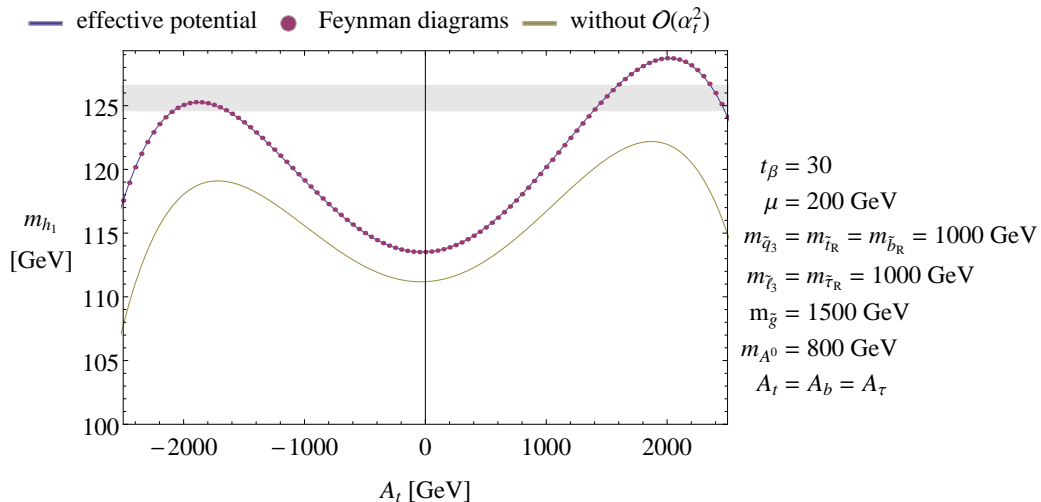


Figure 5. Comparison of the result for the lightest Higgs-boson mass in the effective potential approach (blue) and the Feynman-diagrammatic approach (red). The curves are lying on top of each other, indicating the agreement of both calculations in the limit of real parameters. For reference the result without the contributions of $\mathcal{O}(\alpha_t^2)$ is shown (yellow). The grey area depicts the mass range between 124.6 GeV and 126.6 GeV.

displayed in Fig. 5 underline the importance of the two-loop Yukawa contributions for a reliable prediction of the lightest Higgs boson mass.

In the present version of **FeynHiggs** for complex parameters, the dependence of the $\mathcal{O}(\alpha_t^2)$ terms on the phases of ϕ_{A_t} and ϕ_μ is approximated by an interpolation between the real results for the phases 0 and $\pm\pi$ [23, 35]. A comparison with the full diagrammatic calculation yields deviations that can be notable, in particular for large $|A_t|$. Fig. 6 displays the quality of the interpolation as a function of ϕ_{A_t} and shows that the deviations become more pronounced with rising μ , which is kept real. [Also the admixture of the CP odd part in h_1 is increasing with μ , but it is in general small, below 2%.] The asymmetric behaviour with respect to ϕ_{A_t} is caused by the phase of the gluino mass in the $\mathcal{O}(\alpha_t\alpha_s)$ contributions. The shaded area again illustrates the interval [124.6, 126.6] GeV.

In Fig. 7 the dependence on μ is shown for the mass shift originating from the $\mathcal{O}(\alpha_t^2)$ terms and for the full result for the lightest Higgs-boson mass, choosing different values for the phase ϕ_{A_t} . Particularly for large μ the results can vary significantly and lead to different predictions for the lightest Higgs mass. The kinks around $\mu \approx 1200$ GeV and $\mu \approx 1450$ GeV arise from physical thresholds of the decay of a stop into a higgsino and top.

6 Conclusions

We have presented new results for the two-loop Yukawa contributions $\mathcal{O}(\alpha_t^2)$ from the top–stop sector in the calculation of the Higgs-boson masses of the MSSM with complex parameters. They generalize the previously known result for the real MSSM to the case of complex phases entering at the two-loop level; in the limit of real parameters they confirm the previous result. Combining the new terms with the existing one-loop result and leading two-loop terms of $\mathcal{O}(\alpha_t\alpha_s)$ yields an improved prediction for the Higgs-boson mass spectrum also for complex parameters that is equivalent in accuracy to that of the real MSSM. In the numerical discussion we have focused on the mass of the lightest neutral boson, m_{h_1} , which receives special interest by comparison with the mass of the recently discovered Higgs signal. The mass shifts originating from the $\mathcal{O}(\alpha_t^2)$ terms are

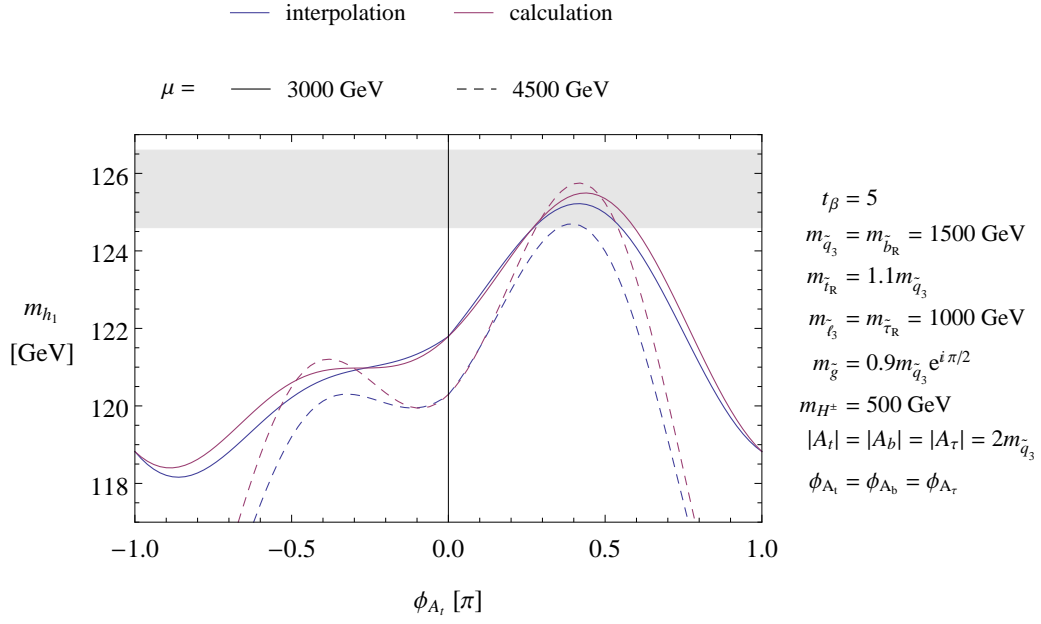


Figure 6. Result from the diagrammatic calculation for complex parameters (red), in comparison with the approximate result from interpolation between the phases $\phi_{A_t} = 0, \pm\pi$. The grey area depicts the mass range between 124.6 GeV and 126.6 GeV.

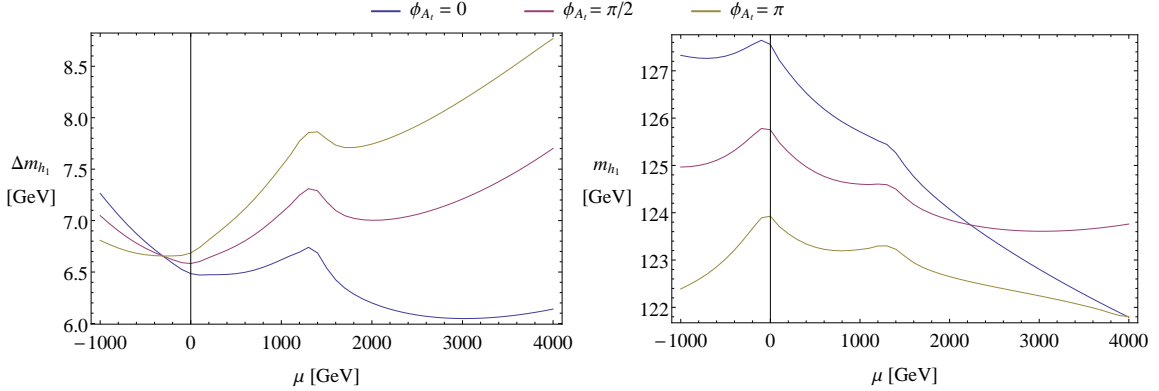


Figure 7. Left: Increasing phase dependence of the $\mathcal{O}(\alpha_t^2)$ contributions to the lightest Higgs-boson mass with rising μ . Right: The lightest Higgs-boson mass including all known contributions. The parameters are chosen as follows: $t_\beta = 7$, $m_{\tilde{q}_3} = m_{\tilde{t}_R} = m_{\tilde{b}_R} = 1500$ GeV, $m_{\tilde{g}} = 1500$ GeV, $m_{H^\pm} = 500$ GeV, $A_t = A_b = A_\tau = 1.6 m_{\tilde{q}_3}$, $m_{\tilde{t}_3} = m_{\tilde{\tau}_R} = 1000$ GeV.

significant, and hence an adequate treatment also for complex parameters is an obvious requirement. The new terms will be included in the code **FeynHiggs**, where so far the complex phases are treated in an approximate way by interpolating between the real results for phases 0 and $\pm\pi$. A more elaborate discussion of the Higgs-boson masses and mixings including the heavier states h_2, h_3 will be given in a forthcoming publication.

Acknowledgement

We thank Stefano Di Vita, Thomas Hahn, Sven Heinemeyer, Heidi Rzehak, Pietro Slavich, Alexander Voigt, and Georg Weiglein for helpful discussions and valuable support.

References

- [1] G. Aad *et al.* [ATLAS Collaboration], Phys. Lett. B **716** (2012) 1 [arXiv:1207.7214 [hep-ex]].
- [2] S. Chatrchyan *et al.* [CMS Collaboration], Phys. Lett. B **716** (2012) 30 [arXiv:1207.7235 [hep-ex]].
- [3] G. Landsberg, talk given at the EPS Conference on High Energy Physics EPS-HEP2013, arXiv:1310.5705 [hep-ex].
F. Cerutti, talk given at the EPS Conference on High Energy Physics EPS-HEP2013, <https://indico.cern.ch/getFile.py/access?contribId=945&sessionId=34&resId=0&materialId=slides&confId=218030>
- [4] A. Pilaftsis, Phys. Rev. D **58** (1998) 096010 [hep-ph/9803297];
A. Pilaftsis, Phys. Lett. B **435** (1998) 88 [hep-ph/9805373].
- [5] J. A. Casas, J. R. Espinosa, M. Quiros and A. Riotto, Nucl. Phys. B **436** (1995) 3 [Erratum-ibid. B **439** (1995) 466] [hep-ph/9407389]. M. S. Carena, J. R. Espinosa, M. Quiros and C. E. M. Wagner, Phys. Lett. B **355** (1995) 209 [hep-ph/9504316].
- [6] S. Heinemeyer, W. Hollik and G. Weiglein, Phys. Rev. D **58** (1998) 091701 [hep-ph/9803277].
S. Heinemeyer, W. Hollik and G. Weiglein, Phys. Lett. B **440** (1998) 296 [hep-ph/9807423].
- [7] S. Heinemeyer, W. Hollik and G. Weiglein, Eur. Phys. J. C **9** (1999) 343 [hep-ph/9812472].
- [8] S. Heinemeyer, W. Hollik and G. Weiglein, Phys. Lett. B **455** (1999) 179 [hep-ph/9903404].
M. S. Carena, H. E. Haber, S. Heinemeyer, W. Hollik, C. E. M. Wagner and G. Weiglein, Nucl. Phys. B **580** (2000) 29 [hep-ph/0001002].
- [9] S. Heinemeyer, W. Hollik, H. Rzehak and G. Weiglein, Eur. Phys. J. C **39** (2005) 465 [hep-ph/0411114].
- [10] R. -J. Zhang, Phys. Lett. B **447** (1999) 89 [hep-ph/9808299]. J. R. Espinosa and R. -J. Zhang, JHEP **0003** (2000) 026 [hep-ph/9912236]. J. R. Espinosa and I. Navarro, Nucl. Phys. B **615** (2001) 82 [hep-ph/0104047]. G. Degrandi, P. Slavich and F. Zwirner, Nucl. Phys. B **611** (2001) 403 [hep-ph/0105096]. R. Hempfling and A. H. Hoang, Phys. Lett. B **331** (1994) 99 [hep-ph/9401219]. A. Brignole, G. Degrandi, P. Slavich and F. Zwirner, Nucl. Phys. B **643** (2002) 79 [hep-ph/0206101]. A. Dedes, G. Degrandi and P. Slavich, Nucl. Phys. B **672** (2003) 144 [hep-ph/0305127].
- [11] J. R. Espinosa and R. -J. Zhang, Nucl. Phys. B **586** (2000) 3 [hep-ph/0003246].
- [12] A. Brignole, G. Degrandi, P. Slavich and F. Zwirner, Nucl. Phys. B **631** (2002) 195 [hep-ph/0112177].
- [13] G. Degrandi, S. Heinemeyer, W. Hollik, P. Slavich and G. Weiglein, Eur. Phys. J. C **28** (2003) 133 [hep-ph/0212020].
- [14] S. Heinemeyer, W. Hollik and G. Weiglein, Phys. Rept. **425**, 265 (2006) [hep-ph/0412214].
- [15] B. C. Allanach, A. Djouadi, J. L. Kneur, W. Porod and P. Slavich, JHEP **0409** (2004) 044 [hep-ph/0406166].
- [16] S. P. Martin, Phys. Rev. D **65** (2002) 116003 [hep-ph/0111209]. S. P. Martin, Phys. Rev. D **66** (2002) 096001 [hep-ph/0206136]. S. P. Martin, Phys. Rev. D **67** (2003) 095012 [hep-ph/0211366]. S. P. Martin, Phys. Rev. D **68** (2003) 075002 [hep-ph/0307101]. S. P. Martin, Phys. Rev. D **70** (2004) 016005 [hep-ph/0312092]. S. P. Martin, Phys. Rev. D **71** (2005) 016012 [hep-ph/0405022]. S. P. Martin, Phys. Rev. D **71** (2005) 116004 [hep-ph/0502168]. S. P. Martin and D. G. Robertson, Comput. Phys. Commun. **174** (2006) 133 [hep-ph/0501132].

- [17] D. A. Demir, Phys. Rev. D **60** (1999) 055006 [hep-ph/9901389]. S. Y. Choi, M. Drees and J. S. Lee, Phys. Lett. B **481** (2000) 57 [hep-ph/0002287]. T. Ibrahim and P. Nath, Phys. Rev. D **63** (2001) 035009 [hep-ph/0008237]. T. Ibrahim and P. Nath, Phys. Rev. D **66** (2002) 015005 [hep-ph/0204092].
- [18] A. Pilaftsis and C. E. M. Wagner, Nucl. Phys. B **553** (1999) 3 [hep-ph/9902371].
- [19] M. S. Carena, J. R. Ellis, A. Pilaftsis and C. E. M. Wagner, Nucl. Phys. B **586** (2000) 92 [hep-ph/0003180].
- [20] S. Heinemeyer, W. Hollik, H. Rzehak and G. Weiglein, Phys. Lett. B **652** (2007) 300 [arXiv:0705.0746 [hep-ph]].
- [21] M. Frank, T. Hahn, S. Heinemeyer, W. Hollik, H. Rzehak and G. Weiglein, JHEP **0702** (2007) 047 [hep-ph/0611326].
- [22] S. Heinemeyer, W. Hollik and G. Weiglein, Comput. Phys. Commun. **124** (2000) 76 [hep-ph/9812320].
- [23] T. Hahn, S. Heinemeyer, W. Hollik, H. Rzehak and G. Weiglein, Comput. Phys. Commun. **180** (2009) 1426.
- [24] S. Dimopoulos and S. D. Thomas, Nucl. Phys. B **465** (1996) 23 [hep-ph/9510220].
- [25] R. D. Peccei and H. R. Quinn, Phys. Rev. Lett. **38** (1977) 1440. R. D. Peccei and H. R. Quinn, Phys. Rev. D **16** (1977) 1791.
- [26] W. Hollik, E. Kraus, M. Roth, C. Rupp, K. Sibold and D. Stockinger, Nucl. Phys. B **639** (2002) 3 [hep-ph/0204350].
- [27] T. Hahn, Comput. Phys. Commun. **140** (2001) 418 [hep-ph/0012260].
- [28] G. Weiglein, R. Scharf and M. Böhm, Nucl. Phys. B **416** (1994) 606 [hep-ph/9310358].
- [29] T. Hahn and M. Perez-Victoria, Comput. Phys. Commun. **118** (1999) 153 [hep-ph/9807565].
- [30] N. Baro, F. Boudjema and A. Semenov, Phys. Rev. D **78** (2008) 115003 [arXiv:0807.4668 [hep-ph]].
- [31] K. E. Williams, H. Rzehak and G. Weiglein, Eur. Phys. J. C **71** (2011) 1669 [arXiv:1103.1335 [hep-ph]].
- [32] A. Freitas and D. Stöckinger, Phys. Rev. D **66** (2002) 095014 [hep-ph/0205281].
- [33] M. Sperling, D. Stöckinger and A. Voigt, JHEP **1307** (2013) 132 [arXiv:1305.1548 [hep-ph]].
- [34] M. Sperling, D. Stöckinger and A. Voigt, arXiv:1310.7629 [hep-ph].
- [35] T. Hahn, S. Heinemeyer, W. Hollik, H. Rzehak and G. Weiglein, arXiv:0710.4891 [hep-ph].